Supporting Information: Trace Organic Gas Analyzer Time-of-Flight mass spectrometer (TOGA-TOF) system for airborne observations of formaldehyde

Daun Jeong[1,a,b], Rebecca S. Hornbrook[2,*], Alan J. Hills[2], Glenn Diskin[3], Hannah S. Halliday[3], Joshua P. DiGangi[3], Alan Fried[4], Dirk Richter[4], James Walega[4], Petter Weibring[4], Thomas F. Hanisco[5], Glenn M. Wolfe[5], Jason St. Clair[5], Jeff Peischl[6,c], Armin Wisthaler[7,8], Tomas Mikoviny[7], John B. Nowak[3], Felix Piel[7], Laura Tomsche[3], Christopher D. Holmes[9], Amber Soja[3], Emily Gargulinski[10], James H. Crawford[3], Jack Dibb[11], Carsten Warneke[12], Joshua Schwarz[12], and Eric C. Apel[2,*]

[1]Advanced Study Program, NSF National Center for Atmospheric Research, Boulder, CO, USA
[2]Atmospheric Chemistry Observations & Modeling Laboratory, NSF National Center for Atmospheric Research, Boulder, CO, USA
[3]NASA Langley Research Center, Hampton, VA, USA
[4]Institute of Arctic and Alpine Research, University of Colorado, Boulder, CO, USA
[5]NASA Goddard Space Flight Center, Greenbelt, MD, USA
[6]Cooperative Institute for Research in Environmental Sciences, University of Colorado, Boulder, CO, USA
[7]Department of Chemistry, University of Oslo, Oslo, Norway
[8]Institute for Ion Physics and Applied Physics, University of Innsbruck, Innsbruck, Austria
[9]Department of Earth, Ocean, and Atmospheric Science, Florida State University, Tallahassee, FL, USA
[10]National Institute of Aerospace, Hampton, VA, USA
[11]Earth Systems Research Center, University of New Hampshire, Durham, NH, USA
[12]Chemical Science Laboratory, National Oceanic and Atmospheric Administration (NOAA), Boulder, CO, USA
[a]now at: Cooperative Institute for Research in Environmental Sciences, University of Colorado, Boulder, CO, USA
[b]now at: Chemical Science Laboratory, National Oceanic and Atmospheric Administration (NOAA), Boulder, CO, USA
[c]now at: Global Monitoring Laboratory, National Oceanic and Atmospheric Administration (NOAA), Boulder, CO, USA

*Corresponding Authors: Eric C. Apel and Rebecca S. Hornbrook
Atmospheric Chemistry Observations & Modeling Laboratory,
NSF National Center for Atmospheric Research, Boulder, CO 80307 USA
apel@ucar.edu
rsh@ucar.edu

Submission to: *Atmospheric Measurement Techniques*
Keywords: FIREX-AQ, formaldehyde, TOGA-TOF, biomass burning

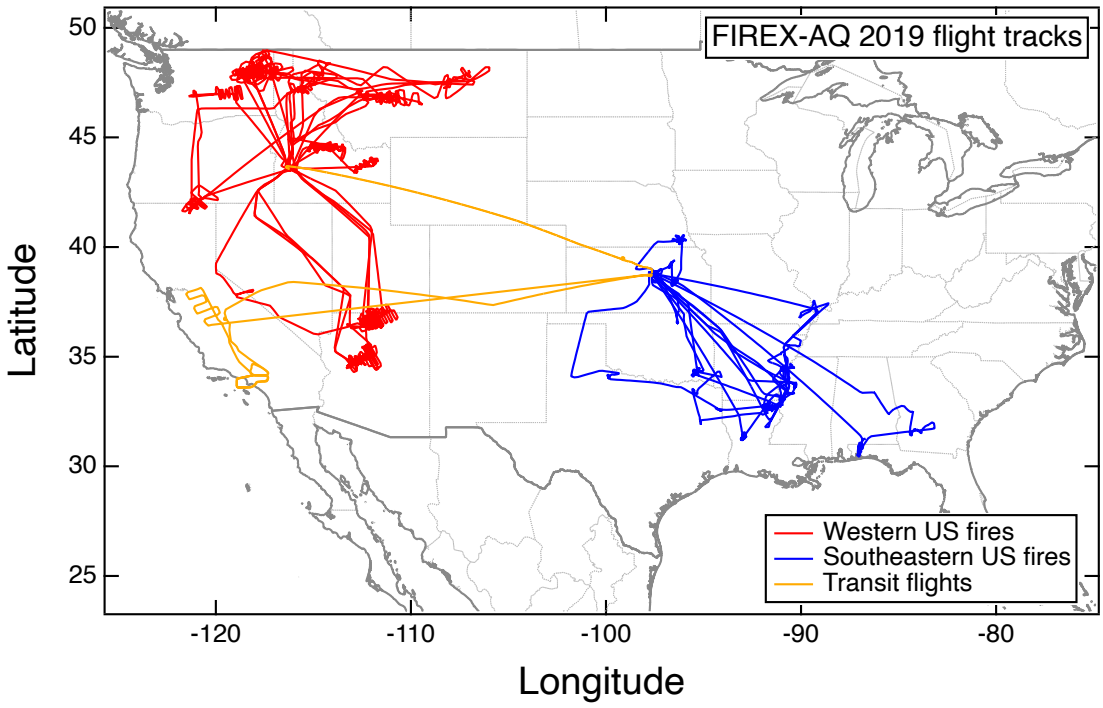

Figure S1. Flight tracks of research and transit flights during FIREX-AQ. Research flights focusing on western wildfires were based in Boise, ID, and research flights focusing on southeastern agricultural fires and prescribed fires were based in Salina, KS.

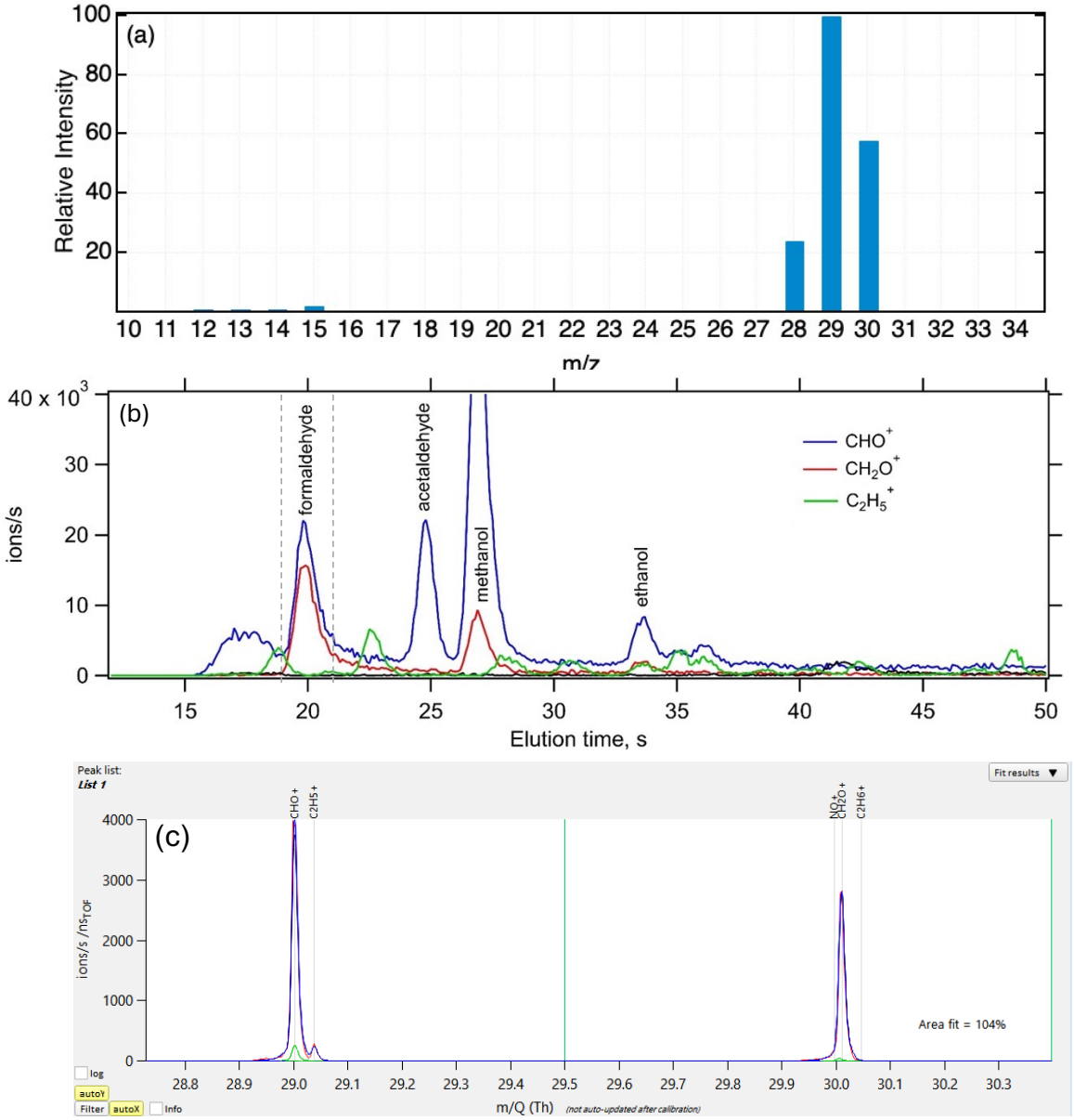

Figure S2. (a) Unit mass fragmentation ions of HCHO with electron ionization (remade from webbook.nist.gov), (b) chromatographic signals of HCHO parent ion CH_2O^+ (m/z 30.010016) and the most dominant fragment CHO^+ (m/z 29.002191), as well as the other major nominal mass 29 ion, $C_2H_5^+$ (m/z 29.038577), and (c) high-resolution peak mass fitting of TOGA-TOF HCHO peak (nominal masses 30 for CH_2O^+ and 29 for CHO^+) at the HCHO elution time (20.2 s) using Tofware (Aerodyne Research, Inc.), showing the mass resolution between CHO^+ and $C_2H_5^+$ and between NO^+ and CH_2O^+.

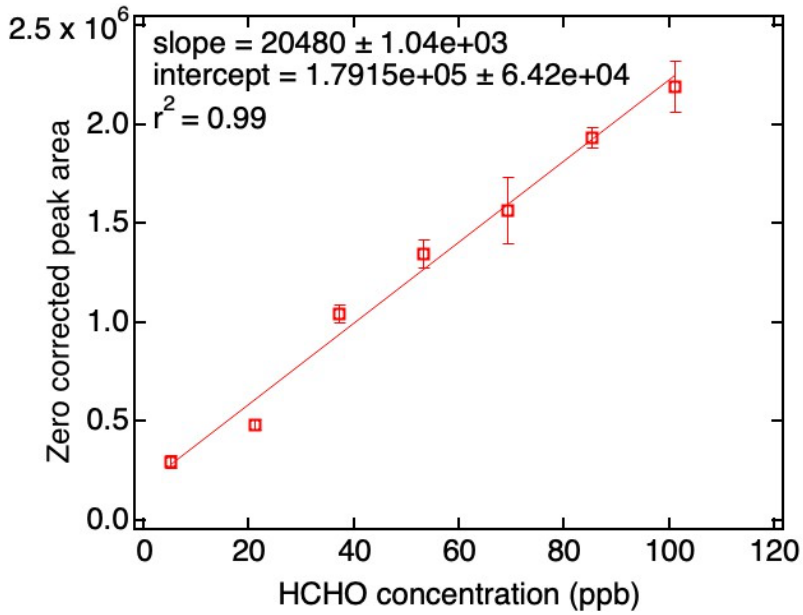

Figure S3. TOGA-TOF HCHO calibration curve, with ODR linear regression of each calibration point. The error bars show the standard error in the repeated peak integration

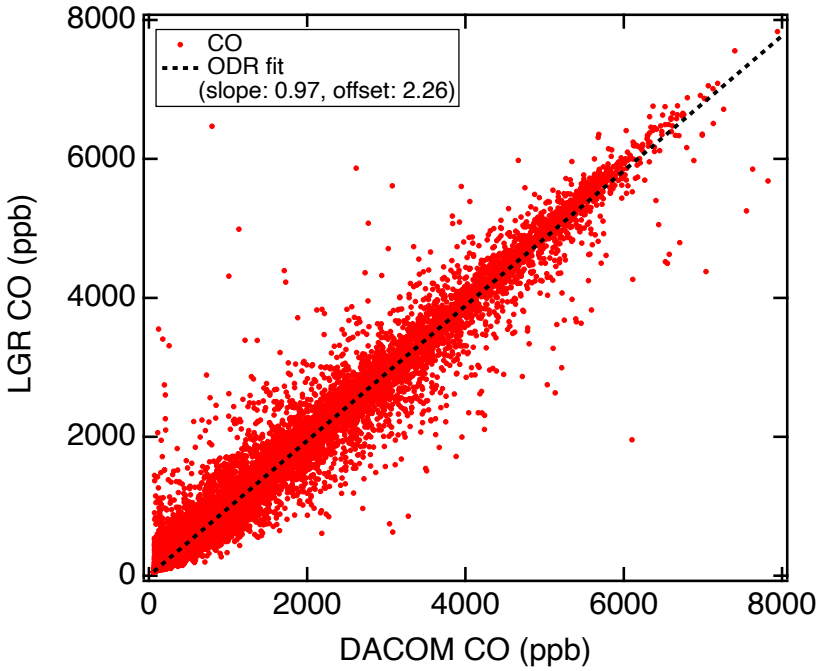

Figure S4. Comparison between 1-Hz CO measured by the LGR and DACOM instruments during FIREX-AQ.

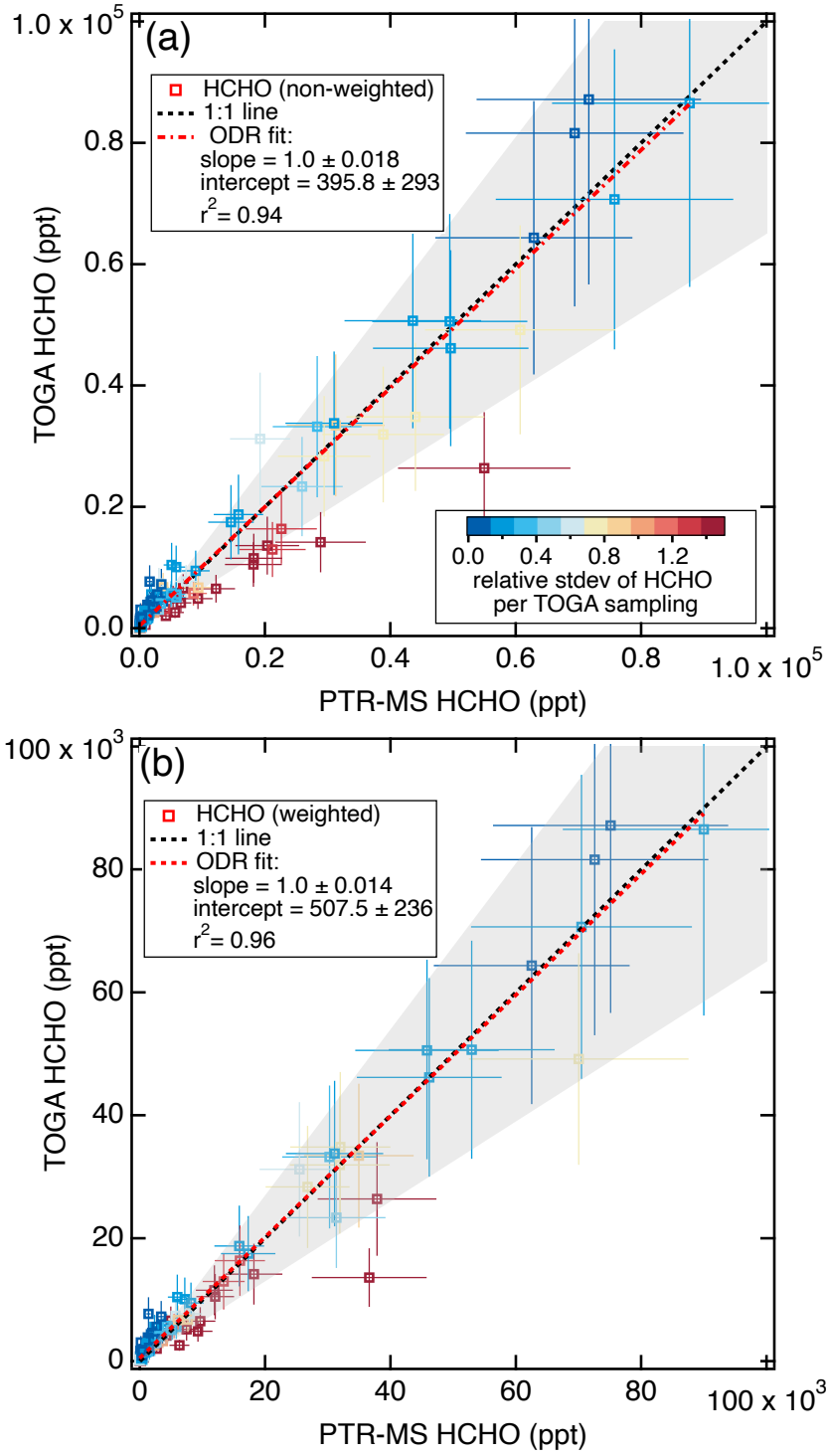

Figure S5. Comparisons between the TOGA-TOF HCHO and the (a) non-weighted and (b) weighted TOGA-merge University of Oslo PTR-MS HCHO. The error bars show the PTR-MS ± 25% accuracy and the TOGA-TOF ± 35% uncertainty.

Table S1. Formaldehyde (HCHO) normalized excess mixing ratios (NEMRs) observed in the western U.S. fire plumes during FIREX-AQ.

Fire name and flight date	Transect start time (UTC)	Transect stop time (UTC)	Physical smoke age (h)[a]	NEMR (HCHO ppt/CO ppb)[b]		
				CAMS	ISAF	TOGA-TOF
Shady 7/25/2019	7/26 00:13:42	7/26 00:17:42	1.2	23.5 ± 0.2	18.1 ± 0.1	15.5 ± 0.8
North Hills 7/29/2019	7/29 23:44:03	7/29 23:49:18	1.3	21.2 ± 0.5	14.9 ± 0.3	12.2 ± 3.1
	7/29 23:52:48	7/29 23:56:18	0.8	13.6 ± 0.4	10.5 ± 0.3	16.4 ± 0.5
	7/30 00:05:03	7/30 00:10:18	1.9	22.4 ± 0.4	17.7 ± 0.3	17.4 ± 2.8
	7/30 00:12:03	7/30 00:17:18	2.4	23.9 ± 0.4	17.8 ± 0.3	20.2 ± 1.4
	7/30 00:19:03	7/30 00:24:18	1.5	19.9 ± 0.5	14.2 ± 0.4	14.4 ± 4.8
	7/30 00:27:48	7/30 00:33:03	2.0	22.2 ± 0.4	15.5 ± 0.3	20.6 ± 0.7
	7/30 00:38:18	7/30 00:43:33	3.4	22.0 ± 0.3	17.2 ± 0.2	18.5 ± 1.1
	7/30 00:45:18	7/30 00:50:33	4.0	23.5 ± 0.4	17.8 ± 0.3	17.9 ± 3.8
Tucker 7/29/2019	7/30 02:44:18	7/30 02:49:33	1.1	19.2 ± 0.2	15.2 ± 0.1	16.9 ± 0.7
	7/30 03:05:17	7/30 03:10:33	1.7	22.0 ± 0.1	17.5 ± 0.1	17.1 ± 0.5
	7/30 03:14:02	7/30 03:19:17	2.1	22.2 ± 0.2	17.6 ± 0.2	18.4 ± 1.8
	7/30 03:21:02	7/30 03:29:48	2.5	21.8 ± 0.2	17.7 ± 0.2	20.5 ± 0.4
	7/30 03:33:18	7/30 03:42:03	3.0	23.7 ± 0.2	18.9 ± 0.1	19.5 ± 1.0
	7/30 03:52:32	7/30 03:57:48	5.4	21.8 ± 0.2	17.6 ± 0.2	19.0 ± 2.1
Lefthand 7/30/2019	7/31 02:12:17	7/31 02:17:32	6.5	21.2 ± 0.4	17.4 ± 0.3	17.9 ± 4.1
	7/31 02:26:16	7/31 02:31:32	7.3	22.6 ± 0.5	16.9 ± 0.3	18.2 ± 3.0
Williams Flats 8/3/2019	8/3 23:07:50	8/3 23:15:35	3.5	14.3 ± 0.06	11.1 ± 0.09	20.3 ± 0.7
	8/3 23:36:18	8/3 23:42:50	3.7	13.4 ± 0.07	10.4 ± 0.1	12.7 ± 0.7
	8/3 23:46:20	8/3 23:51:00	3.8	11.4 ± 0.2	9.0 ± 0.2	13.8 ± 2.1
	8/4 00:33:01	8/4 00:37:55	0.6	15.2 ± 0.1	11.8 ± 0.1	15.7 ± 0.3
	8/4 00:37:55	8/4 00:44:38	1.7	16.7 ± 0.05	12.8 ± 0.07	12.4 ± 2.2
	8/4 00:44:38	8/4 00:49:53	1.7	18.4 ± 0.1	14.3 ± 0.09	17.9 ± 0.5
	8/4 01:00:26	8/4 01:09:11	2.1	18.2 ± 0.06	13.9 ± 0.06	12.2 ± 0.7
	8/4 01:10:56	8/4 01:16:11	2.6	19.9 ± 0.04	15.3 ± 0.08	18.8 ± 0.4
	8/4 01:17:56	8/4 01:22:12	2.9	19.8 ± 0.07	15.3 ± 0.1	22.2 ± 0.4
	8/4 01:30:57	8/4 01:36:12	2.4	21.0 ± 0.07	16.3 ± 0.1	22.7 ± 1.0
	8/4 01:39:42	8/4 01:43:12	3.1	19.9 ± 0.07	15.4 ± 0.1	17.9 ± 0.8
	8/4 01:51:57	8/4 01:55:27	4.0	20.2 ± 0.06	15.9 ± 0.1	18.7 ± 0.4
Williams Flats 8/7/2019	8/8 00:41:17	8/8 00:44:47	2.0	19.1 ± 0.2	15.1 ± 0.1	21.0 ± 0.2
	8/8 01:11:02	8/8 01:20:12	0.7	17.3 ± 0.1	13.7 ± 0.08	19.4 ± 1.4
	8/8 01:41:20	8/8 01:46:35	2.1	19.2 ± 0.2	15.2 ± 0.1	23.3 ± 0.9
	8/8 01:48:20	8/8 01:53:35	2.5	20.1 ± 0.1	15.8 ± 0.1	23.9 ± 0.2
	8/8 01:57:05	8/8 02:02:20	2.8	20.2 ± 0.1	15.9 ± 0.1	21.6 ± 0.5
	8/8 02:07:35	8/8 02:12:50	3.3	21.0 ± 0.2	16.6 ± 0.1	24.1 ± 0.3
Williams Flats 8/8/2019	8/9 00:53:00	8/9 00:58:15	2.5	16.4 ± 0.3	13.7 ± 0.2	11.8 ± 0.7
	8/9 01:11:59	8/9 01:17:14	0.9	11.6 ± 0.2	9.2 ± 0.1	13.9 ± 0.2
	8/9 01:20:44	8/9 01:25:59	1.1	12.5 ± 0.3	10.2 ± 0.2	12.0 ± 0.8
	8/9 01:31:14	8/9 01:35:54	1.2	12.6 ± 0.4	10.5 ± 0.2	20.2 ± 0.3
	8/9 02:09:57	8/9 02:15:12	2.0	14.0 ± 0.2	11.6 ± 0.1	15.2 ± 0.04
	8/13 00:16:26	8/13 00:19:56	0.5	19.1 ± 0.1	16.4 ± 0.3	20.1 ± 0.3

Castle 8/12/2019	8/13 00:25:11	8/13 00:28:41	1.0	19.3 ± 0.1	16.0 ± 0.2	17.6 ± 0.5
	8/13 00:32:11	8/13 00:37:26	1.0	19.2 ± 0.08	16.0 ± 0.1	16.0 ± 0.5
	8/13 00:40:56	8/13 00:46:07	1.6	19.6 ± 0.07	16.2 ± 0.1	22.6 ± 0.5
	8/13 00:59:00	8/13 01:06:00	3.4	22.4 ± 0.1	18.4 ± 0.1	23.2 ± 0.5
	8/13 01:11:15	8/13 01:20:00	3.6	22.0 ± 0.2	17.8 ± 0.1	21.1 ± 1.1
	8/13 01:20:00	8/13 01:27:00	3.1	18.5 ± 0.1	15.5 ± 0.1	19.5 ± 1.2
	8/13 01:32:15	8/13 01:39:15	4.2	21.8 ± 0.2	18.7 ± 0.1	22.2 ± 0.5
	8/13 01:41:00	8/13 01:49:45	4.7	22.8 ± 0.1	18.9 ± 0.1	20.2 ± 1.8
	8/13 01:51:30	8/13 01:58:30	5.5	21.4 ± 0.2	17.4 ± 0.1	20.3 ± 0.9
	8/13 02:00:15	8/13 02:09:00	5.7	22.6 ± 0.2	18.4 ± 0.1	20.1 ± 0.6
	8/13 02:10:45	8/13 02:17:45	6.0	21.5 ± 0.3	17.6 ± 0.2	20.1 ± 2.3
	8/13 03:06:45	8/13 03:10:15	1.5	16.9 ± 0.3	13.8 ± 0.4	13.4 ± 0.3
	8/13 03:12:00	8/13 03:17:15	2.8	19.2 ± 0.06	15.3 ± 0.1	17.3 ± 1.3
	8/13 03:20:45	8/13 03:28:29	3.5	19.9 ± 0.06	15.5 ± 0.09	19.4 ± 3.4
	8/13 03:28:29	8/13 03:33:51	2.4	18.9 ± 0.1	14.2 ± 0.1	23.7 ± 1.4
Castle 8/13/2019	8/13 23:39:57	8/13 23:46:57	2.7	21.9 ± 0.2	18.8 ± 0.2	22.7 ± 0.3
	8/13 23:48:42	8/13 23:57:27	2.8	23.1 ± 0.1	19.4 ± 0.1	24.0 ± 1.2
	8/13 23:59:12	8/14 00:07:57	3.2	24.5 ± 0.2	20.5 ± 0.1	25.5 ± 0.7
	8/14 00:09:42	8/14 00:20:12	3.2	26.1 ± 0.1	21.5 ± 0.1	26.8 ± 1.4
	8/14 00:20:12	8/14 00:30:42	3.3	26.6 ± 0.2	22.0 ± 0.2	29.7 ± 1.9
	8/14 00:32:27	8/14 00:44:42	3.2	27.1 ± 0.09	22.5 ± 0.1	29.7 ± 1.4
	8/14 00:46:27	8/14 00:56:57	3.7	22.8 ± 0.2	19.0 ± 0.2	23.0 ± 2.0
	8/14 01:38:11	8/14 01:45:10	1.7	20.0 ± 0.1	16.8 ± 0.2	21.3 ± 0.5
	8/14 01:51:26	8/14 01:54:58	2.2	23.2 ± 0.2	20.0 ± 0.3	16.8 ± 2.1
	8/14 02:07:13	8/14 02:14:13	2.4	22.8 ± 0.1	18.6 ± 0.1	22.0 ± 0.5
	8/14 02:15:57	8/14 02:22:57	3.3	24.1 ± 0.1	20.1 ± 0.1	24.3 ± 1.0
	8/14 02:26:27	8/14 02:35:12	3.6	25.0 ± 0.1	20.9 ± 0.1	26.3 ± 1.1
	8/14 02:35:12	8/14 02:45:42	4.1	25.4 ± 0.08	21.3 ± 0.1	28.3 ± 2.3
	8/14 02:47:28	8/14 02:57:58	4.7	26.5 ± 0.1	22.1 ± 0.1	27.0 ± 1.1
	8/14 02:57:58	8/14 03:11:58	5.6	26.7 ± 0.09	22.4 ± 0.1	29.2 ± 1.6
Sheridan 8/16/2019	8/17 00:38:52	8/17 00:43:42	0.3	15.8 ± 0.3	13.6 ± 0.2	19.0 ± 0.1
	8/17 00:47:11	8/17 00:52:37	0.4	16.4 ± 0.2	14.7 ± 0.1	20.8 ± 0.01
	8/17 00:54:22	8/17 01:00:08	0.5	16.8 ± 0.3	15.1 ± 0.2	23.1 ± 0.9
	8/17 01:01:53	8/17 01:06:22	0.7	17.6 ± 0.2	15.6 ± 0.1	18.3 ± 0.3
	8/17 01:08:07	8/17 01:13:25	0.8	17.4 ± 0.1	15.6 ± 0.1	21.6 ± 0.2
	8/17 01:13:25	8/17 01:20:19	1.2	18.6 ± 0.2	17.0 ± 0.1	22.5 ± 0.7
	8/17 01:23:49	8/17 01:29:04	1.2	18.9 ± 0.1	17.0 ± 0.1	18.3 ± 0.3
	8/17 01:29:04	8/17 01:36:04	1.5	19.8 ± 0.2	17.8 ± 0.2	20.7 ± 1.9
	8/17 01:39:34	8/17 01:46:34	1.6	22.3 ± 0.2	19.7 ± 0.2	22.4 ± 0.6
	8/17 01:48:19	8/17 01:55:19	2.3	22.5 ± 0.1	20.3 ± 0.1	22.8 ± 0.7
	8/17 02:14:34	8/17 02:30:19	3.2	23.0 ± 0.1	20.7 ± 0.1	22.4 ± 0.9
	8/17 02:30:19	8/17 02:46:04	4.1	23.2 ± 0.1	20.8 ± 0.2	24.3 ± 1.1
	8/17 03:38:34	8/17 03:54:19	4.2	22.7 ± 0.2	20.4 ± 0.1	26.0 ± 3.0
	8/17 03:54:19	8/17 04:08:19	3.8	23.3 ± 0.2	20.9 ± 0.2	26.6 ± 2.8
	8/17 04:10:04	8/17 04:27:34	4.6	20.4 ± 0.2	19.0 ± 0.1	22.0 ± 1.4

[a]The physical smoke ages shown are the median values of the 1-s physical smoke age for each transect based on mean winds, neglecting plume rise, as reported by J. P. Schwarz in the FIREX-AQ website (https://www-air.larc.nasa.gov/missions/firex-aq/).

[b]The slope of the HCHO and CO measurements between the transect start and stop time was used to calculate each NEMR. NEMR uncertainties shown are the uncertainties in the slope of the linear least-squares fits to the data.